

# Contribution of surface state characterization to studies of works of art

Mady Elias,\* Caroline Magnain, and Jean Marc Frigerio

Institut des Nanosciences de Paris, UMR CNRS 7588, Université Pierre et Marie Curie,  
140 rue de Lourmel, 75015 Paris, France

\*Corresponding author: mady.elias@insp.jussieu.fr

Received 22 December 2009; revised 9 March 2010; accepted 16 March 2010;  
posted 16 March 2010 (Doc. ID 121853); published 7 April 2010

This paper has two purposes. The first one underlines that qualitative and quantitative studies of surface states lead to relevant information for analyzing works of art, with lots of potential for art history, restorers, and curators. The discrimination between different artistic techniques and the influence of a varnish on the leveling of paint surfaces are presented. The second purpose is the comparison between different nondestructive optical topographic methods, i.e., goniophotometry, optical coherence topography, and confocal microscopy, according to their accuracy, their discriminatory ability, their practicability inside a museum, and the size limits of the studied objects. © 2010 Optical Society of America

*OCIS codes:* 030.5770, 100.6950, 240.6700, 290.1350, 180.1655, 180.1790.

## 1. Introduction

The surface states of works of art strongly influence their visual appearance. An increase of the roughness involves a bleaching of the colored surface that induces colorimetric variations, such as an increase of the lightness and a decrease of the saturation [1]. At the same time, the gloss decreases. The surface state can be a fingerprint of the masterpiece [2] and sometimes of the artist's production. Its recording can be a part of the archiving of the collection in a museum. It can also be a tool for drawing up a status report before and after an exhibition or a loan and for the fight against forgery [3]. The modification of the surface state can be due to a restoration or to specific conditions of conservation or exhibitions and must be checked during the follow-up and the monitoring of conservation or restoration treatments [4–7]. Finally, surface metrology is also a method able to identify some artistic techniques that stand out by their roughness [8,9]. Topographic information is then very important in the field of art for art historians, restorers, and curators.

To study unique works of art, the experimental methods must be nondestructive and contactless. Optics in the visible range is then a prioritized field and allows establishing the link between gloss and surface topography. Previous studies have already been published, each focusing on a particular artistic case and using a given optical instrument [2–8]. Imaging is prioritized in these studies and quantitative surface characteristics are rarely provided. In this paper, we propose to compare different optical methods with the intent of making an easier choice in a future application. The comparison is not exhaustive, but refers to the instruments developed at Institut des Nanosciences de Paris (INSP) or in a European project. For a quantitative comparison of the results, theoretical bases of surface metrology are recalled in the Section 2. Three instruments are then presented in Section 3: a goniophotometer in a backscattered configuration, optical coherence tomography (OCT) in the visible range, and a portable confocal microscope. Specular and distinctness-of-image (DOI) glossmeters are also quickly described.

Various applications in art are presented in the Section 4. They always cross surface state with visual appearance. First, the discrimination between the three gold application techniques (on a bole, on

a mixture, and in an eggshell paint), which differ by their roughness, is described. An example of this identification is presented in an altarpiece from the 16th century. Second, the influence of the binder (oil, egg tempera, wax milk, caparol, and cellulose) on the surface state of paintings is developed. It is applied to the comparison of the artistic techniques used in the representation of complexion according to the epoch, from the 2nd century to now. Finally, the leveling of a paint layer by a varnish is studied. Both surface states of the varnish and of the paint layer are simultaneously recorded by different methods and compared. This application could lead to the development of new synthetic varnishes according to the request of artists and restorers.

These examples will be the opportunity to present, in Section 5, a comparison between the previous methods used for imaging or quantifying the surface states. Their accuracy, but also their discriminatory ability, their practicability inside a museum, and the size limits of the studied objects are then considered.

## 2. Theoretical Basis

To compare the results obtained with different instruments, common relevant characteristics must be defined. All the studied surfaces of works of art are here considered as random. Their topography is then characterized by two geometrical quantities [10]:

- the root mean square (r.m.s.) roughness  $h = \sqrt{\langle z^2 \rangle}$  deduced from the surface function  $z(x)$  or  $z(x, y)$ , describing the height  $z$  of the surface referred to its mean plane, along a line or in a whole plane, and
- the correlation length  $l$  defined by the correlation function  $C(\epsilon) = \langle z(x + \epsilon)z(x) \rangle \approx h^2[1 - (\epsilon/l)^2]$ , with its approximation in the case of an isotropic surface.

The r.m.s. roughness and the correlation length of the studied surfaces are always larger than the wavelengths in the visible range. The surfaces are then classified as strongly rough in this range. Moreover, when the radius of curvature  $\rho \approx h^2/l$  is smaller than the wavelength, which is here justified, the sur-

faces can be decomposed in a series of plane microfacets [11]. By definition,  $(h/l_x)^2 = \langle (\partial z / \partial x)^2 \rangle$  and  $(h/l_y)^2 = \langle (\partial z / \partial y)^2 \rangle$ . In the case of an isotropic surface,  $l_x = l_y$ . Let  $(\theta, \varphi)$  be the angles of the normal to a microfacet, then  $(\partial z / \partial x) = \tan \theta \cos \varphi$  and  $(\partial z / \partial y) = \tan \theta \sin \varphi$ . It follows that  $(h/l)^2 = (1/2) \langle \tan^2 \theta \rangle$ . The ratio  $h/l$  is then the relevant geometric characteristic of the surface state [10]. It will be chosen for comparing the results obtained with different instruments. The larger this ratio, the rougher is the corresponding surface.

## 3. Experimental Techniques

Common requirements in studying unique works of art are to use nondestructive, contactless, portable instruments, leading to rapid analysis *in situ*. We describe successively three optical devices for studying the surface states: goniophotometry, OCT, and confocal microscopy, presented in Fig. 1. A glossmeter is also shortly described, in order to link topography and visual appearance.

### A. Goniophotometry in Backscattered Configuration

The specificity of the portable goniospectrophotometer is its back-scattered configuration [Fig. 1(a)]. This configuration is of great interest for surface state studies and is also employed in lidar, radar, and sonar techniques for studying topography, but with other wavelength ranges. In the setup developed at INSP [10], two beams of optical fibers are randomly mixed. The first one illuminates the studied surface with white light. The second one collects the light backreflected by this surface with the same angle. The analyzed surface is a disk with a 5 mm diameter, large enough to ensure statistical results with correlation length at the micrometer scale. The radiance  $L(\theta)$  is measured for different backscattered angles, adjusted by a goniometer, averaged on negative and positive angles, and then normalized by its maximum  $L_{\max}$ . The normalized radiance  $L_{\text{norm}}(\theta) = L(\theta)/L_{\max}$  is wavelength quasi-independent because the variation of the refractive index is smaller than 2% in the visible range. The measurements are then realized for a given wavelength. The normalized radiance is then directly proportional to the probability

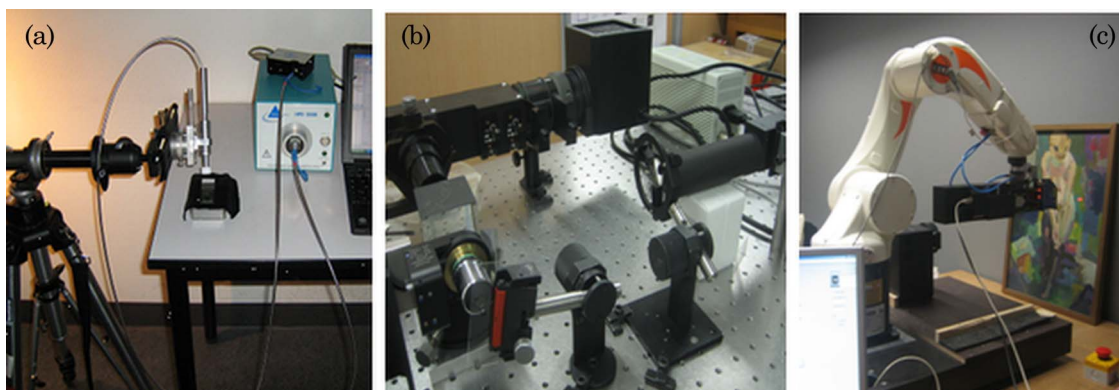


Fig. 1. (Color online) Three different instruments used in this study: (a) a goniospectrophotometer in backscattered configuration, (b) a full-field and time-domain OCT in the visible range, and (c) a portable confocal microscope  $\mu\text{surf}$  (Nanofocus AG), mounted on a robot.

density of the slopes of the microfacets  $P_N$ , normalized by  $\iint P_N d\Omega = 1$ . The more angularly spread the curve, the rougher is the surface. A perfect plane surface will theoretically lead to a Dirac function for  $\theta = 0^\circ$ , with a perfect collimated incident beam. In the experimental setup, it defines the angular accuracy. The curve  $L_{\text{norm}}(\theta)$  then allows easily deducing the ratio  $h/l$ , using

$$\left(\frac{h}{l}\right)^2 = \frac{1}{2} \langle \tan^2 \theta \rangle = \frac{1}{2} \frac{\int \int \tan^2 \theta L_{\text{norm}}(\theta) d\Omega}{\int \int L_{\text{norm}}(\theta) d\Omega}.$$

This process has already been validated by comparison of the ratio  $h/l$  obtained by goniophotometry and profilometry on several rough copper surfaces [10]. The respective accuracy of  $L_{\text{norm}}$  is  $\pm 0.05$  and of  $\theta$  is  $\pm 0.5^\circ$ . The ratio  $h/l$  is deduced within  $\pm 0.01$ .

#### B. Optical Coherence Tomography

OCT has already been implemented in the infrared range and in the Fourier domain for studying topography of works of art [4,7]. A full-field OCT in the time domain has been recently developed at INSP, working in the visible range [12,13] [Fig. 1(b)]. Its first specificity is the working domain in the visible range chosen for future spectral pigment identification in stratified layers. Its second specificity is the use of a Mirau interferometric objective that avoids moving the studied surface. Moreover, this Mirau objective decreases the sensitivity to vibrations. It also increases the contrast of the images by use of various splitter reference surfaces with different reflectivity. It supplies today two-dimensional (2D) and three-dimensional (3D) en-face and cross-sectional images.

To define a profile  $z(x)$  from the OCT images, the following method is implemented. At each lateral location  $x$ , the interface is first considered as thick and located in the  $z$  range where the gray level is larger than 98% of its maximum value.  $z(x)$  is then defined as the mean value of  $z$  in this range. After that, the profile is redressed and the r.m.s. roughness  $h$  is deduced. The correlation function is calculated and the correlation length  $l$  is deduced by the first zero crossing of this function. Finally, the ratio  $h/l$  is calculated, with a rather low accuracy, due to the optical noise of the image.

The spatial resolution is around  $1\ \mu\text{m}$  for the three directions, as for more classical OCT working in the IR range. The ratio  $h/l$  is deduced within  $\pm 0.05$ . The lateral size of the images is around  $320\ \mu\text{m}$  today without any scanning with a  $\times 20$  magnification of the Mirau objective. The analyzed depth stands around  $50\ \mu\text{m}$ , depending on the pigment concentration. The instrument will be portable in the near future.

#### C. Confocal Microscopy

A white-light confocal microscope  $\mu\text{surf}$  developed by Nanofocus [14] is used in this study. It has already been implemented for particular studies of works of art [3,5,6], but only with a qualitative point of view.

The instrument allows measurements of areas up to  $1\ \text{mm}^2$  in size without stitching, with a lateral accuracy down to  $1\ \mu\text{m}$ , and a vertical one of around  $0.2\ \mu\text{m}$  by use of relatively low magnification ( $\times 20$ ). 2D and 3D en-face and cross-sectioning images are provided, but on the condition that the upper layer is transparent, in contrast with OCT. Profiles with low noise are deduced from the images. The ratio  $h/l$  is then simply calculated, using  $(h/l)^2 = \langle (\partial z / \partial x)^2 \rangle$  with an accuracy of around 0.01. This vertical accuracy can reach 10 nm with higher magnification, but smaller studied areas, and is rarely useful for studies on works of art. The depth penetration can be  $100\ \mu\text{m}$  for transparent media. The microscope is now portable and mounted on a robot [3], as shown in Fig. 1(c).

#### D. Gloss Measurements

To link topography and visual appearance, we also implement gloss measurements. For the varnish study, specular gloss at  $20^\circ$ ,  $60^\circ$ , and  $85^\circ$  was determined using a micro-TRI-gloss instrument [15]. The measured quantity is defined by  $G(\theta) = 100L_{\text{sample}}(\theta)/L_{\text{ref}}(\theta)$ , where  $L_{\text{ref}}(\theta)$  is the radiance reflected by a reference standard, a highly polished planar black glass with a refractive index equal to 1.567. The accuracy of  $G(\theta)$  is in the 1%–2% range. For the binder influence, specular gloss measurements are implemented with a ZLR 1050 developed by Zehntner at  $20^\circ$ ,  $60^\circ$ , and  $75^\circ$ . Finally, Distinctness-of-Image (DOI) gloss is determined according to ASTM International E 430 using a Dorigon II abridged goniophotometer [15]. The measured quantity is now defined by  $\text{DOI} = 100(L_{\text{sample}}(30^\circ) - L_{\text{sample}}(30^\circ \pm 0.3^\circ))/L_{\text{sample}}(30^\circ)$ . The rougher the studied surface, the smaller is the specular gloss and the larger is the DOI gloss. Specular gloss and DOI accuracy lie around 10% and the studied surface is about  $1\ \text{cm}^2$ . The instruments are portable, but some need contact.

### 4. Applications in Art

#### A. Discrimination of the Gold Application Techniques

Three different artistic techniques of gold application are found in the literature [16] and attested from cross sections of samples taken on real works of art and using electronic microscopy. The first technique is called “gold on a mixtion.” An oleo-resinous medium is first applied on the background; the gold leaf is then put on it. The medium dries slowly and the gold leaf cannot be polished. The final metallic surface is then strongly rough. This technique is mostly employed in Byzantine and Orthodox icons. The second technique is called “gold on a bole.” The gold leaf is applied on an aqueous binder where pigments, such as ochre, are embedded. This medium dries quickly and the gold leaf can be polished. The final surface is less rough. This technique is mostly employed in religious Italian primitive paintings. The last technique is the eggshell paint technique,

in which gold particles are embedded in a binder. The paint is applied in thin layers without any polishing. This technique leads to the roughest surface. It is commonly used in manuscripts but also in some European easel paintings. Although the three methods differ by their final roughness, visual observation cannot easily discriminate among them, as shown in Fig. 2. The restoration intervention, evidently, depends on the technique and only roughness measurements can be used to distinguish among them, if no sampling is allowed.

In this case, only goniophotometry in a backscattered configuration is used for the discrimination. Figure 3 shows the normalized radiance  $L_{\text{norm}}(\theta)$  measured on three model samples corresponding to the three previous techniques. The process has also been reproduced many times on real paintings for which the gold application technique was already known. The ratio  $h/l$  corresponding to the precious curves are presented in Table 1. Graphs and ratio  $h/l$  allow a satisfactory discrimination among the three techniques.

The same process has been applied to study the golden column of the angels' concert, painted by Matthias Grünewald in the 16th century, presented in Fig. 4. The studied panel belongs to a triptych, which is hung 4 m high, and the platform allowed only a lightweight instrument. Only goniophotometry was then implementable. The results on the column are added in Fig. 3 and in Table 1. They have been reproduced in ten different locations of the two columns. Both the curves and the ratio  $h/l$  underline a column realized with a gold leaf on a mixtion. This information is first interesting for the choice of a future restoration intervention. The layer under the gold leaf is an oleo-resinous medium and will determine the chemical products used for the intervention. This result also supplies information for

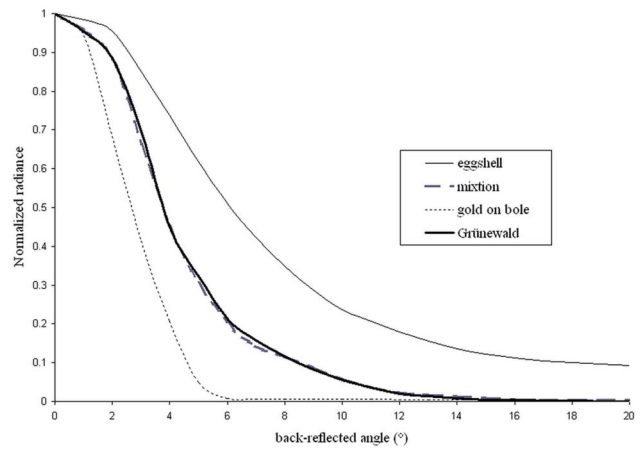


Fig. 3. Goniophotometry in backscattered configuration: normalized radiance  $L_{\text{norm}}$  as a function of the backscattered angle  $\theta$  for the three different gold application techniques and for the golden column of Grünewald's altarpiece presented on Fig. 4.

art history on Grünewald's artistic process. This gold leaf on a mixtion underlines a new influence of Grünewald's realization coming from Northern Europe, which adds to other Italian inspirations highlighted by the drawing and the iconography of the altarpiece.

#### B. Influence of the Binder on the Surface States of Paintings

The works of art more often present painted dielectric surfaces than metallic ones. This study then focuses on the different artistic techniques used for the representations of complexions in easel paintings, according to the epochs. From the literature [17,18] and numerous pigment identifications on real paintings, it can be deduced that the pigments used by the artists, from the 2nd century to the 19th century, were almost the same: burnt umber or



Fig. 2. (Color online) Examples of different gold application methods: (a) gold on a mixtion, Russian icon, 15th century; (b) gold on a bole, Virgin, Giovanni di Paolo, 15th century; and (c) eggshell paint, manuscript, 15th century.

**Table 1. Ratio  $h/l$  as a Function of the Different Gold Techniques**

Surface	Gold on a Bole	Gold on a Mixtion	Eggshell Paint	Grünewald
$h/l$	$0.03 \pm 0.01$	$0.06 \pm 0.01$	$0.14 \pm 0.01$	$0.07 \pm 0.01$

vermillion and lead white. Only the binders vary with the epoch: wax, tempera (with glue or egg), oil, caparol, and cellulose binders were successively employed and led to different visual effect. To only change the nature of the binder and to keep the same pigment and the same volume pigment concentration, samples of “complexions” have been realized by a contemporary artist, Jean Pierre Brazs. We here present the results on samples made of burnt umber and, successively, the five different binders. Other pigments or pigment mixtures have been studied in the same way to investigate the influence of the binder on the visual appearance.

Goniophometry, OCT, and specular gloss measurements have been implemented on the corresponding samples [19]. Goniophotometric results are presented in Fig. 5. The studied surfaces are no longer metallic, as in the previous application, but also scattering, and the contribution of the bulk scattering

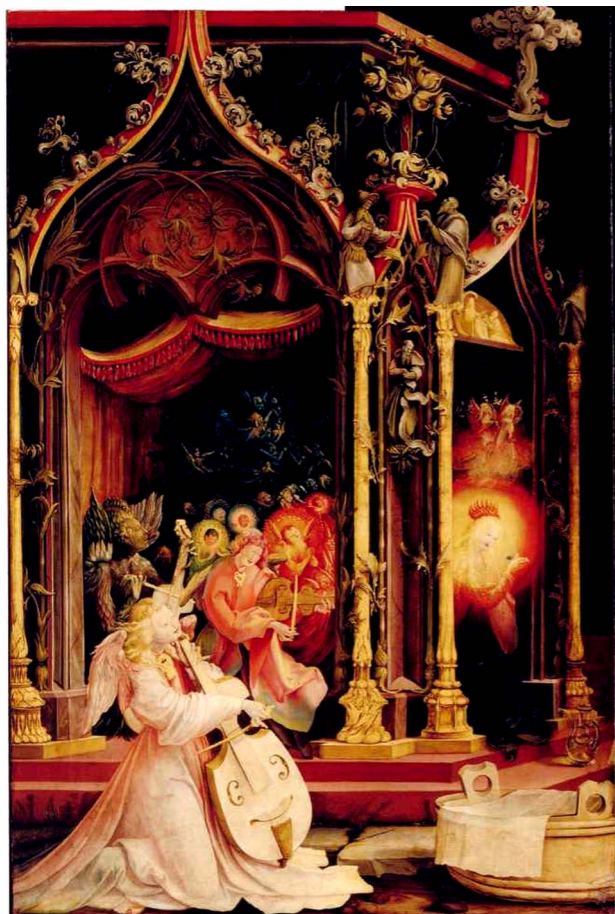


Fig. 4. (Color online) The angels' concert, part of the Isenheim's altarpiece by Grünewald (16th century), Unterlinden Museum, Colmar, France.

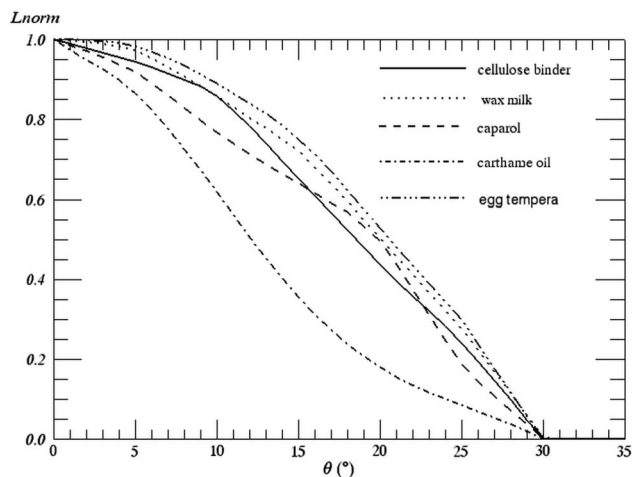


Fig. 5. Goniophometry in backscattered configuration: normalized radiance as a function of the backscattered angle for samples made of burnt umber and different binders.

(radiance over  $30^\circ$ ) has been subtracted. Nevertheless, the nature and the concentration of the pigments are the same in all the samples; the bulk scattering is then similar and the results can be compared among themselves. This light scattering also explains the difference between the shape of the curves of Figs. 3 and 5 and no serious comparison can be deduced from these figures. The corresponding ratios  $h/l$  are presented in Table 2. Goniometry clearly distinguishes the oil binder from the others. The carthame oil leads to the narrowest curve and to the smallest  $h/l$  ratio, thus to a smoother surface. The other binders are all aqueous and goniophotometry cannot discriminate them.

OCT has also been implemented and we present the results on two samples. The 2D cross sections are presented in Fig. 6. They clearly show a smooth surface for the carthame oil binder and a rough surface for the cellulose binder. The ratios  $h/l$ , obtained after removing the noise, are presented in Table 2 and they are accordance with the goniometric results.

Finally, specular gloss measurements have been implemented on the same samples at different angles. The results are gathered in Table 2. As expected, gloss increases when the roughness and the ratio  $h/l$  decrease. Only large reflection angles ( $75^\circ$ ) allow discrimination between some binders. Actually, the Fresnel reflection coefficient increases with the specular angle and then the accuracy on the gloss increases, also.

The three different kinds of measurements show the same results: the oil binder creates a smoother surface than all the other aqueous binders; the ratio  $h/l$  is the smallest and the specular gloss is the largest. Nevertheless, the gloss at  $75^\circ$  discriminates more clearly this binder from the aqueous ones than the ratio  $h/l$  (a multiplicative factor equal to 10 instead of 2). The aqueous binders lead to rather similar surface states and cannot be easily discriminated. In this case, the ratio  $h/l$  is more discriminating than

Table 2. Ratio  $h/l$  and Specular Gloss for Different Angles and Different Binders [19,20]

Binder	$h/l$ OCT	$h/l$ Goniophotometry	Specular Gloss at 20°	Specular Gloss at 60°	Specular Gloss at 75°
Cellulose	$0.15 \pm 0.05$	$0.09 \pm 0.01$	$0.5 \pm 0.1$	$0.6 \pm 0.1$	$0.9 \pm 0.1$
Wax milk		$0.10 \pm 0.01$	$0.5 \pm 0.1$	$0.6 \pm 0.1$	$0.6 \pm 0.1$
Caparol		$0.09 \pm 0.01$	$0.5 \pm 0.1$	$0.6 \pm 0.1$	$0.7 \pm 0.1$
Carthame oil	$0.10 \pm 0.05$	$0.07 \pm 0.01$	$0.7 \pm 0.1$	$3.6 \pm 0.1$	$11.9 \pm 0.1$
Egg tempera		$0.10 \pm 0.01$	$0.4 \pm 0.1$	$0.7 \pm 0.1$	$1.3 \pm 0.1$

the gloss at 75° (a relative variation of 25% instead of 15%). The evaporation of the solvent during the drying of the aqueous paintings, associated to the migration of the pigments toward the surface, generates final rough surfaces. On the other hand, the evaporation of the solvent in an oil binder is weak and very slow. These different evaporations can certainly explain the difference between the final surface states of oil and aqueous paintings.

These results are now at the art historians' disposal, in order to explain how these different binders and their visual appearance answer to the fashion or to the queries of the epoch or to the ease of use for the artists.

### C. Leveling of the Paint Layer by a Varnish

If the binder influences the surface state of a painting, then the applying of a varnish also modifies the final topography and the visual appearance by leveling the paint surface. For this study, natural varnishes with different aging, different resins, and different backgrounds are used to quantify the surface state characteristics of each interface (air/varnish and varnish/background). The results are compared with previous studies on synthetic varnishes that underline the influence of the molecular weight of the resin on this leveling [15,20].

Confocal microscopy allows simultaneous imaging of both interfaces of a varnished object and cross sections including these interfaces. These images lead to the measurement of the varnish thickness, to the r.m.s. roughness, to the correlation length of each interface, and to the ratio  $h/l$ . We present here one example on a hand-made painted surface covered by a fresh varnish made of mastic and turpentine. We have obtained similar results with other resins (dammar), with different states of degradation, with other binders (linseed oil or a mixture of linseed oil and turpentine), and with other backgrounds (metal or glass). A cross section of the sample is shown in Fig. 7, where both interfaces are visible. The total depth is 90  $\mu\text{m}$  and the lateral dimension is 800  $\mu\text{m}$ . This cross

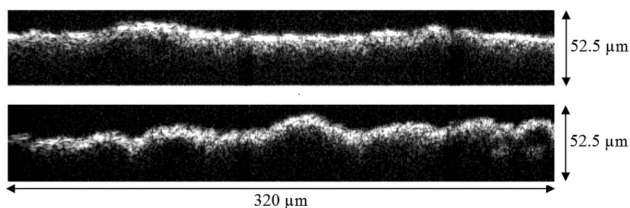


Fig. 6. OCT cross sections for samples made of a burnt umber and cellulose binder (down) and burnt umber with carthame oil (top).

section can be compared with the OCT results obtained on the same sample and shown in Fig. 8. The micrometric accuracy is the same for both devices. The leveling of the paint by the varnish is clearly visible on the OCT and confocal images. Both images also show that the measurement of the varnish thickness can only be an average. By example, on the confocal image, an axis (arrow) is chosen on the cross section and a depth profile can be deduced along this axis. The distance between the peaks, corresponding to the light reflected by both interfaces, allows deducing the varnish thickness, here around 24  $\mu\text{m}$ , but only relevant along this axis. In this hand-made case, the brush strokes are visible and the varnish thickness can be evaluated between 0 and 40  $\mu\text{m}$ .

Confocal microscopy also allows simultaneous imaging of both interfaces of the same sample in 2D or 3D, as shown in Figs. 9(a) and 9(b). The size of the recorded surface is 800  $\mu\text{m} \times 800 \mu\text{m}$ . Corresponding profiles are deduced along any chosen direction. The profiles of both interfaces along a diagonal are presented in Figs. 10(a) and 10(b). These profiles lead to quantitative results for each interface, obtained from ten bordering profiles end to end and presented in Table 3. As expected, the paint surface is actually more than 32 times rougher than the varnish upper surface. The brush strokes of the hand-made paint layer are clearly distinguishable in Figs. 7–10. Moreover, it must be noticed from the profiles [Figs. 10(a) and 10(b)] that the varnish levels the high spatial frequencies of the paint and that only

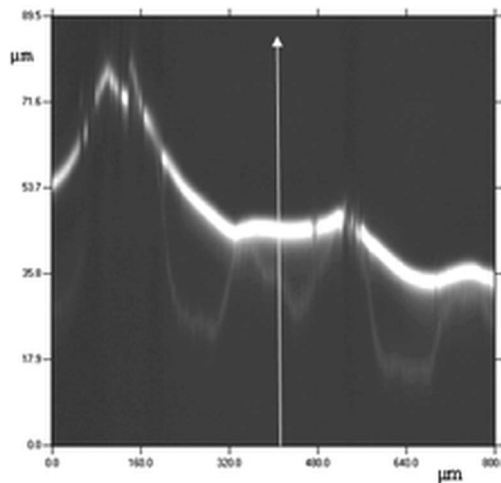


Fig. 7. Confocal microscopy cross section on a paint sample varnished with a fresh mastic in turpentine.

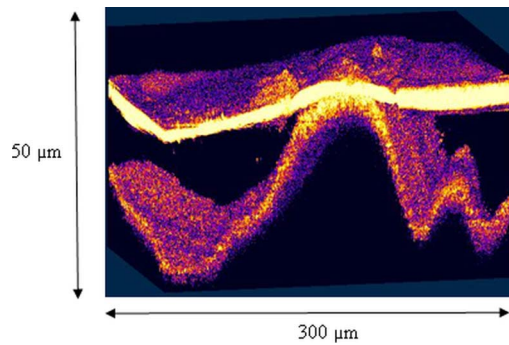
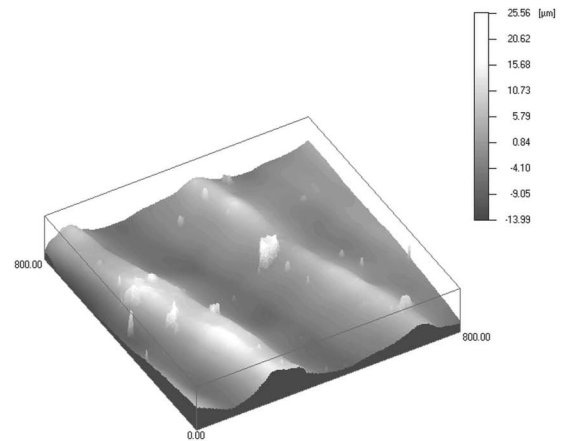


Fig. 8. (Color online) OCT cross section in 3D of a paint sample varnished with a fresh mastic in turpentine [12].

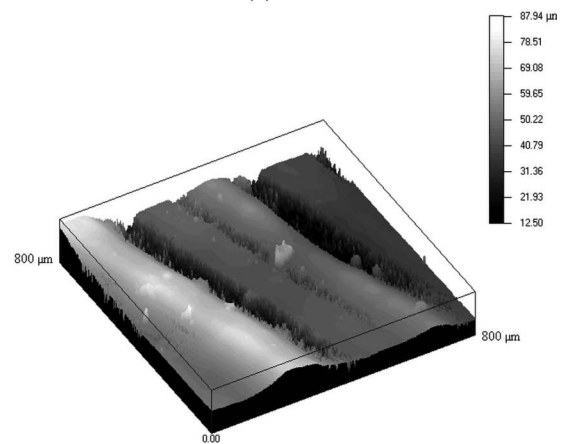
the brush strokes of the paint remain in the upper interface. The high frequencies belonging to the second interface can be due to the drying of the hand-made paint (rising of the pigments toward the surface), but also to some experimental artifacts of the instrument (narrow oscillations with sudden break slopes). Nevertheless, this particular spatial filtering has already been underlined on synthetic varnishes and glass backgrounds and quantified by Fourier transform and power spatial distribution [20]. Other varnishes, backgrounds, and states of degradation lead to similar results.

These results can be compared to those obtained previously [15,20] by use of a stylus profilometer and a glossmeter, on two synthetic varnishes, AYAT and Regalrez, applied on a rough glass plate. These varnishes have been studied for quantifying the influence of the molecular weight of the resin contained in the varnish on the leveling effect. AYAT has a high molecular weight and Regalrez has a low molecular weight. The r.m.s. roughness, correlation length, and ratios  $h/l$  deduced from the profiles are gathered in Table 4. The varnish strongly reduces the roughness of the background in mineral varnishes. The ratio between the varnish roughness and the background is 7 times larger in the case of synthetic varnishes, due to different techniques of application (an applicator instead of a brush). The influence of the molecular weight of the resin is clearly underlined for synthetic varnishes: the leveling by the Regalrez, a resin with a small molecular weight, is much more important than by the AYAT, with its large molecular weight. Finally, the spatial filtering previously observed for mineral varnishes is also noticeable in the profiles of synthetic varnishes and is more pronounced for low molecular weight resins.

We finish this study by comparing specular and DOI gloss measurements of these synthetic varnishes with the previous topographic results. The results have been added in Table 4. As expected, specular and DOI glosses increase when the roughness of the varnished surface decreases and, therefore, when the molecular weight of the resin decreases. We also notice that DOI gloss is more discriminating than specular gloss.



(a)



(b)

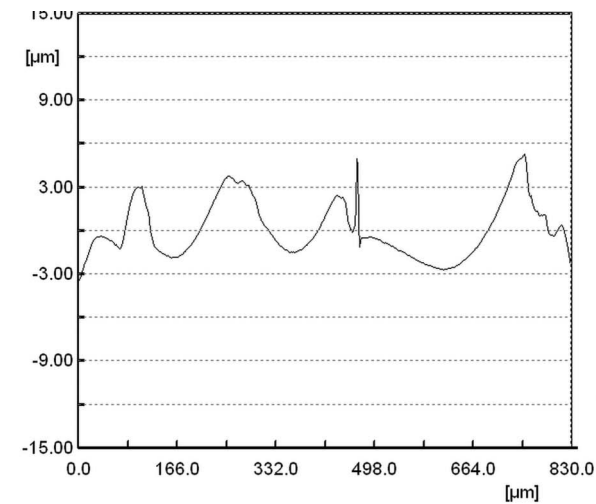
Fig. 9. (a) 3D confocal image of the air/varnish interface of the same sample. (b) 3D confocal images of the varnish/paint interface of the same sample.

These results will allow the development of a panel of new varnishes with various glosses, by varying the molecular weight of the synthetic resin and according to the request of artists and restorers.

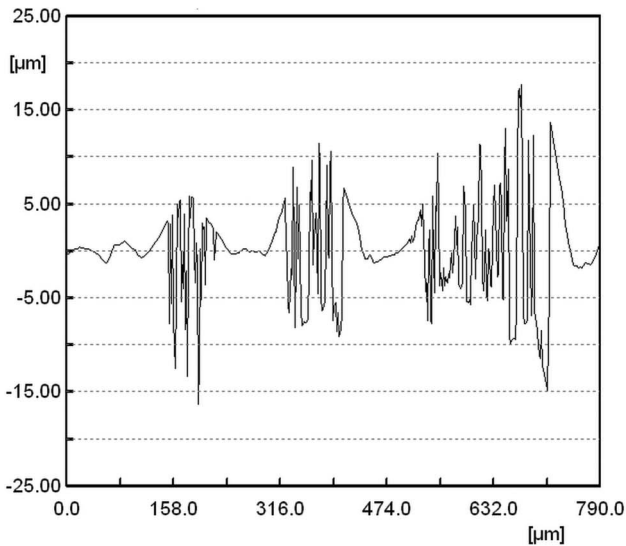
## 5. Discussion

We here compare the different methods previously described, for their application to the study of works of art. All the described instruments can now be implemented with daylight and do not need any sampling. To distinguish among themselves, several criteria must then be taken into account: the ease of implementation, the graphic interpretation of the results, the relevance of the quantitative results, and their accuracy, of course.

In a first step, gloss measurements can be used before topographic inspection. It is the easiest technique for implementation. Relevant information can be supplied for comparative studies, such as the discrimination among different artistic techniques or materials. For specular gloss, large angles must be prioritized. DOI must be preferred to specular gloss, for a better discrimination. Both gloss measurements



(a)



(b)

Fig. 10. (a) Profile of the interface air/varnish of the same sample along a diagonal of the en-face confocal image of Fig. 9(a). (b) Profile of the interface varnish/paint of the same sample along a diagonal of the en-face confocal image [Fig. 9(b)].

have accuracy of around  $\pm 0.05$ . Nevertheless, if the standard setups are portable, they often need contact with the studied surfaces.

In a second step, goniophotometry in a backreflected configuration supplies graphic information, easily interpretable for the discrimination among different artistic techniques. The results are directly obtained from the measured radiance and no further computational image processing is then needed. Quantitative values of the ratio  $h/l$  can be deduced

for quantification of the geometrical characteristics of the studied surfaces and for further comparison, with accuracy around 0.01, such as for the following methods. The studied area is a 5 mm diameter disk. The setup is lightweight (around 1 kg), contactless, easily portable, and easy to use inside the museum. It is adaptable to any position of the studied surface, thanks to a ball joint and a translation table. The implementation is relatively fast, around some minutes. An automation of the goniometer rotation could be a possible improvement. This method supplies only results of the upper interface of the objects and must be kept for comparison among different artistic productions. The process does not provide images for archiving.

For the imaging of interfaces and cross sections, confocal microscopy is also relatively fast to implement and can now be used inside a museum, thanks to a robot. The important advantage, compared to a classical profilometer, is the possibility of simultaneously recording both interfaces of both sides of a transparent layer (varnish). Signal processing is then needed to obtain the 2D and 3D images and statistical processing from the deduced profiles is needed for quantification of the surface states, in opposition to the goniophotometric method. The accuracy on  $h/l$  is  $\pm 0.01$ , as for goniophotometry, but here  $h$  and  $l$  can be separately deduced with  $\pm 0.1 \mu\text{m}$ . It is also a tool to deduce a varnish thickness from cross sections, which cannot be obtained by goniophotometry. This method is well adapted for fingerprint and archiving, and for qualitative and quantitative comparative studies. An important improvement will take into account the recorded surface function  $z(x, y)$ , allowing direct deduction of the ratio  $h/l$  without the assumption of an isotropic surface, as it is done from linear profiles. A second improvement, in progress today, is the stitching of images and profiles in order to increase the size of the studied surfaces. A last improvement will deal with reducing of robot's weight, which does not allow today a measurement from scaffolding.

Finally, OCT results lead to the same micrometric accuracy in the three directions, the same depth limit, of around  $50 \mu\text{m}$ , the same surface area, around some hundreds of micrometers square, and similar images to those obtained by confocal microscopy. The main difference deals with the imaging of scattering media, which is possible with OCT. Both coupled information on topography of the interfaces and on pigment imaging and identification will be of major interest for the study of works of art. The same improvements described for confocal microscopy are foreseen with OCT: processing of the surface function

Table 3. Topographic Characteristics of Both Interfaces of the Same Sample, Deduced from Previous Confocal Profiles

Interface	r.m.s. Roughness $h$ ( $\mu\text{m}$ )	Correlation Length $l$ ( $\mu\text{m}$ )	$h/l$
Air/varnish	$2.0 \pm 0.1$	$16.6 \pm 0.1$	$0.12 \pm 0.01$
Varnish/paint	$4.8 \pm 0.1$	$16.6 \pm 0.1$	$0.29 \pm 0.08$

**Table 4. Topographic Characteristics and Gloss of Two Synthetic Varnishes, AYAT and Regalrez, Applied on a Rough Glass [19,20]**

Sample	Glass (Background)	Glass + AYAT	Glass + Regalrez
r.m.s. roughness $h$ ( $\mu\text{m}$ )	$0.7 \pm 0.1$	$0.08 \pm 0.03$	$0.02 \pm 0.01$
Correlation length $l$ ( $\mu\text{m}$ )	$2.5 \pm 0.2$	$1.3 \pm 0.4$	$0.4 \pm 0.1$
Ratio $h/l$	$0.28 \pm 0.02$	$0.06 \pm 0.01$	$0.05 \pm 0.01$
Specular gloss at $30^\circ$		$0.57 \pm 0.06$	$0.85 \pm 0.08$
DOI gloss at $30^\circ$		$0.23 \pm 0.02$	$0.90 \pm 0.09$

and stitching of the images. The instrument is not yet portable but will be set up on a robot in a microscope rack in the near future.

## 6. Conclusion

Using different experimental methods, we have presented three particular studies of topography applied to works of art.

We first show that different artistic techniques of gold application (on a mixtion, on a bole, and in egg-shell paint) can be discriminated by their final roughnesses without any sampling. It leads to a guess of the nature of the binder under the gold leaf. Gold on a mixtion has then been identified *in situ* on an altarpiece painted by Grünewald. This kind of identification is useful both for choosing the materials used in a future restoration and for the knowledge of art history and of the geographic influences of the artist.

We then present the influence of different binders (oily or aqueous) used by the artists according to the epoch, to paint “complexions” in easel paintings. The visual appearance of these artistic techniques differs and is mainly linked to various surface states. The oil binder is distinguishable from others by a smoother surface and an important gloss. Aqueous binders lead to rather similar surface states and visual appearances. These results are now devoted to art history by explaining the reasons of this evolution.

We finished by the study of the leveling of a paint surface by different varnishes. The role of the molecular weight of the resin is underlined: the smaller the molecular weight, the more important is the leveling of the background, while the smaller the roughness and the ratio  $h/l$ , the larger is the specular and the DOI gloss. An immediate application of these results is the possible follow-up of varnish removal during a restoration and a tool for deciding the beginning or the ending of such an intervention. Another important application of this study is the development of a panel of new varnishes with various glosses, by varying the molecular weight of the synthetic resin, according to the request of artists and restorers.

In conclusion, this comparative study shows that the imaging and the quantification of surface states are powerful tools for studying works of art. We must add that these surface states and their modulations are also a powerful subject of creation in art, as in the “ultra-black” paintings of the contemporary French artist Pierre Soulages.

## References

1. L. Simonot and M. Elias, “Color change due to surface state modification,” *Color Res. Appl.* **28**, 45–49 (2003).
2. European Project 022453—Sixth Framework Programme Priority 8.1.B.3.6. “Fingartprint,” <http://www.technologyreview.com/Infotech/18241/?a=f>.
3. W. Wei, P. Boher, M. Elias, J. Frohn, K. Martinez, and S. Sotiropoulou, “A new non-contact fingerprinting method for the identification and protection of objects of art and cultural heritage against theft and illegal trafficking,” in *Proceedings of the 7th European Conference “SAUVEUR”—Safeguarded Cultural Heritage—Understanding & Viability for the Enlarged Europe*, M. Drdacky and M. Chapuis, eds. (European Community, 2006), pp. 103–111, <http://www.arcchip.cz/ec-conference/proc.php>.
4. P. Targowski, R. Ostrowski, J. Marczak, M. Sylwestrzak, and E. A. Kwiatkowska, “Picosecond laser ablation system with process control by optical coherence tomography,” *Proc. SPIE* **7391**, 73910G (2009).
5. W. Wei, S. Stangier, and A. De Tagle, “In situ characterisation of the surface of paintings before and after cleaning using white light confocal profilometry,” in *Proceedings of Art '05*, 8th International Conference on Non-destructive Investigations and Microanalysis for the Diagnostics and Conservation of the Cultural and Environmental Heritage, Lecce, Italy, 15–19 May 2005.
6. P. Ravines, C. M. Wichern, and J. Chen, “Optical and surface metrology to study cultural heritage: confocal topometry applied to the surface study of photographic images,” in *Proceedings of Art '08*, 9th International Conference on Non-Destructive Testing of Art, Jerusalem, 25–30 May 2008.
7. D. C. Adler, J. Stenger, I. Gorczynska, H. Lie, T. Hensick, R. Spronk, S. Wolohojian, N. Khandekar, J. Y. Jiang, S. Barry, A. E. Cable, R. Huber, and J. G. Fujimoto, “Comparison of three-dimensional optical coherence tomography and high resolution photography for art conservation studies,” *Opt. Express* **15**, 15972 (2007).
8. R. I. Grynspan, J. L. Pastol, S. Lesko, E. Paris, and C. Raepsaet, “Surface topology investigation for ancient coinage assessment using optical interferometry,” *Appl. Phys. A* **79**, 273–276 (2004).
9. W. J. Stemp and M. Stemp, “Documenting stages of polish development on experimental Stone tools: surface characterization by fractal geometry using UBM laser profilometry,” *J. Archaeol. Sci.* **30**, 287–296 (2003).
10. M. Elias and M. Menu, “Experimental characterization of a random metallic rough surface by spectrophotometric measurements in the visible range,” *Opt. Commun.* **180**, 191–198 (2000).
11. P. Beckmann and A. Spizzichino, *The Scattering of Electromagnetic Waves from Rough Surfaces*, ed. (Pergamon, 1963).
12. G. Latour, J. P. Echard, B. Soulier, I. Emond, S. Vaiedelich, and M. Elias, “Structural and optical properties of wood and wood finishes using optical coherence tomography: application to an 18th century Italian violin,” *Appl. Opt.* **48**, 6485–6491 (2009).

13. G. Latour, J. Moreau, M. Elias, and J. M. Frigerio, "Optical coherence tomography: non-destructive imaging and spectral information of pigments," *Proc. SPIE* **6618**, 661806 (2007).
14. [www.nanofocus-us.com/index.php?id=16](http://www.nanofocus-us.com/index.php?id=16).
15. R. De La Rie, M. Elias, and J. Delanay, "The role of varnishes in modifying light reflection from rough surfaces—a study of changes in light scattering caused by variations in varnish topography and development of a drying model," *Stud. Conserv.* **53**, 170–186 (2009).
16. L. Tintori, "Golden tin in Sienese murals of early trecento," *Burlington Mag.* **74**(2), 94–96 (1982).
17. Pliny the Elder, *The Natural History*, J. Bostock, H. T. Riley, eds. (Taylor and Francis, 1855), Book 35, Chap. 1.
18. M. Théophile, *An Essay Upon Diverse Arts* (c. 1125) translation, J. G. Hawthorne and C. C. S. Smith, eds. (Dover, 1979).
19. C. Magnain, M. Elias, and J. M. Frigerio, "Influence of the artistic techniques on the visual appearance of complexions in art," *Proc. SPIE* **7391**, 739108 (2009).
20. M. Elias, R. De La Rie, J. Delanay, and E. Charron, "Leveling of varnishes over rough substrates," *Opt. Commun.* **266**, 586–591 (2006).